

LASER ANGLE OF INCIDENCE EFFECTS ON IN-SITU CONSOLIDATION OF AUTOMATED FIBER PLACEMENT OF POLYARYLEETHERKETONE COMPOSITES

Brian W. Grimsley¹, Tyler B. Hudson¹, Roberto J. Cano¹, Jamie C. Shiflett², Christopher J. Stelter¹, Christopher J. Wohl¹, Rodolfo I. Ledesma³, Thammaia Sreekantamurthy³, Jin Ho Kang¹, John P. Nancarrow⁴, Ryan F. Jordan⁴, and Jake H. Rower⁴

¹NASA Langley Research Center, Hampton, VA 23681

²KBRWyle, Inc., Hampton, VA 23681

³Analytical Mechanics Associates, Inc., Hampton, VA 23681

⁴Electroimpact, Inc., Mukilteo, WA 98275

ABSTRACT

NASA and Electroimpact, Inc. ^{®††} in conjunction with other U.S. industry partners are performing research as a part of the NASA High-rate Composites for Aircraft Manufacturing (HiCAM) Project to fabricate thermoplastic panels using automated fiber placement (AFP) to increase manufacturing rates of aircraft structural composites. This work focuses on evaluating the in-situ consolidation AFP of thermoplastics (ICAT) process. Previous studies of the ICAT process using semi-crystalline, polyaryletherketone (PAEK) slit-tape have resulted in an adequate degree of intimate contact between plies; however, the resulting interlaminar strength have been less than laminates fabricated in an autoclave. To improve these properties, the effect of reducing the laser angle of incidence (AoI) during placement to increase the degree of auto-hesion was evaluated. The AoI of the laser assisted AFP head was varied between 12° and 16° to fabricate multiple quasi-isotropic and unidirectional test panels. Physics-based thermal models developed at the NASA Langley Research Center were utilized to predict the temperature profile. Laminate processing temperature was measured experimentally, and panel quality was evaluated by both non-destructive evaluation (NDE) as well as destructively by photo-microscopy. The effect on interlaminar strength was determined by short beam strength testing. Test results of carbon fiber laminates fabricated by ICAT using polyetheretherketone (PEEK), polyetherketoneketone (PEKK), and low-melt polyaryletherketone (LM-PAEK) at various laser angles of incidence, placement temperatures and placement speeds are presented.

Keywords: thermoplastic composites, automated fiber placement, laser heating

Corresponding author: Brian W. Grimsley; brian.grimsley@nasa.gov

SAMPE Paper Submittal #: TP24-0000000178

Copyright C: This paper is declared a work of the U.S. Government and is not subject to copyright protection in the United States.

††Specific vendor and manufacturer names are explicitly mentioned only to accurately describe the hardware used in this study. The use of vendor and manufacturer names does not imply an endorsement by the U.S. Government, nor does it imply that the specified equipment is the best available.

*SAMPE Conference Proceedings. Long Beach, CA May 20-23, 2024.
Society for the Advancement of Material and Process Engineering – North America.*

1. INTRODUCTION

1.1 Thermoplastic AFP

NASA has partnered with the U.S. aerospace industry and academia on the HiCAM project, initiated in 2021 to evaluate and develop high-rate manufacturing of composite primary airframe structure for commercial aircraft. The goal of the project is to increase the manufacturing throughput of composite fuselage and wing shipsets by six times the current baseline (2020 technology) to meet projected market demands for future single-aisle aircraft of up to 80 aircraft per month with reduced cost and no weight penalty. Thermoplastic (TP) matrix composites are inherently suitable for rapid manufacturing due to their formability at elevated temperatures and because full consolidation can be achieved without the long autoclave cure cycle required for the cross-linking chemical reaction of thermoset (TS) matrix composite structure. The semi-crystalline polyaryletherketone (PAEK) family of linear aromatic TP polymers, including PEEK, PEKK, and LM-PAEK result in composite laminates which boast several advantages over thermoset composites, including comparable mechanical performance to toughened epoxy matrix composites over the operating temperature range of commercial aircraft [1], improved fracture toughness [2], high chemical and moisture resistance, and the potential for recyclability. In addition, the use of carbon fiber (CF) reinforced TP in production eliminates the need for freezer storage associated with uni-tape TS matrix composites. Further, creep associated with the PAEK polymer matrix composites is consistent with toughened epoxy composites [3]. The high-rate production potential of CF/PAEK composites has been demonstrated for processes such as stamp-forming and continuous compression molding (CCM) [4] to fabricate aerospace structure of constant cross-section such as beams, stringers and frames. The reason these processes can achieve full consolidation and mechanical property development in a matter of minutes as opposed to the hours required for autoclave cure of TS matrix composites is due to the nature of the healing and auto-hesion process associated with welding, or healing, of the thermoplastic polymer matrix. The healing of a thermoplastic polymer is described below in Figure 1.

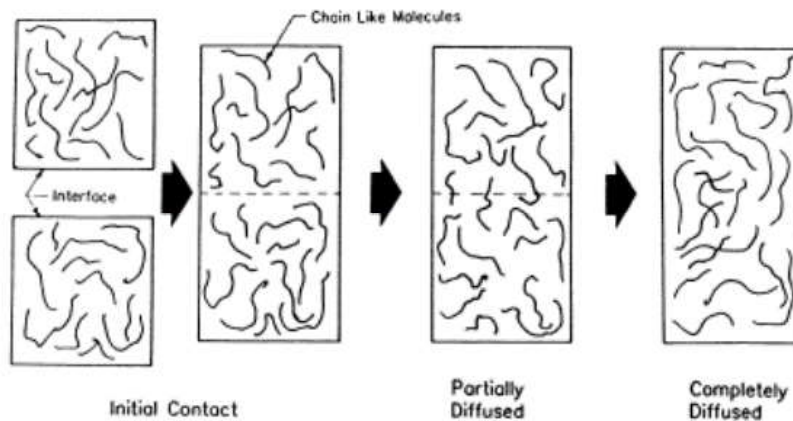


Figure 1: Schematic of thermoplastic fusion bonding (auto-hesion) phenomenon.

Thermoplastic matrix composites can be consolidated and welded very quickly due to auto-hesion. As shown in Figure 1, the steps involved include first establishing intimate contact between the two surfaces to be fused together; these surfaces can be two plies in a laminate stack or the welding of a stringer to a wing skin. Intimate contact is established when the two surfaces are heated above the crystalline melt temperature (T_M). Loos and Springer [5] characterized the squeeze-flow of a molten CF/ thermoplastic material under a compaction load and developed a physics-based model

to predict the time required to establish intimate contact related to the viscosity of the polymer and the surface irregularities, or surface roughness, of the tape. Depending on the surface roughness, temperature and viscosity of the tape surface polymer, intimate contact can be established in less than one second under adequate compaction pressure. After intimate contact is established, the mechanical strength of the interface is developed through the process of auto-hesion governed by diffusion and the reptation theory of Degennes [6]. Above T_M , the long-chain polymer molecules can reptate, or randomly slide past one another bridging the interface to penetrate and entangle in polymer molecules on the other side of the interface. The strength of the interface is governed by the diffusion time at the given temperature. Wool [7,8] developed an isothermal welding model for amorphous thermoplastics (Equation 1), relating the time required to develop strength of the cohesive bond to adequate auto-hesion and polymer molecule interpenetration. The dependence of the average molecule interpenetration depth is calculated as a function of time, using reptation dynamics. The average molecule interpenetration depth is the important molecular feature during the healing process of the amorphous thermoplastic molecules and is also applicable to semi-crystalline polymers above T_M :

$$\frac{\sigma}{\sigma_{\infty}} = t^{\frac{1}{4}} M^{-\frac{3}{4}} \quad (1)$$

Where, $\frac{\sigma}{\sigma_{\infty}}$ is the ratio of the cohesive strength, σ , to ultimate strength of the pristine polymer, σ_{∞} , t is the time the interface is in intimate contact above the T_M , and M is the weight average molecular weight of the polymer, which can be characterized experimentally. Wool's welding model indicates that the linear relationship between strength and time to the one quarter power is followed until the cohesive strength of the material is attained. This phenomenon explains how processes like stamp-forming and CCM result in composite laminates with autoclave comparable properties after only seconds of compaction load applied to the part above the T_M . While these processes offer significant rate reduction for certain structural elements on commercial aircraft, they are not suitable for the fabrication of large acreage primary structure such as wing or fuselage skin. To address the manufacture of these larger parts, the HiCAM project is evaluating the automated fiber placement (AFP) process commonly utilized to place CF reinforced TS slit-tape on rigid tooling followed by a consolidation step in either autoclave or under a vacuum bag in an oven (VBO). The AFP process is a computer aided manufacturing (CAM) technique inherently providing the capability to create a faster production process and composite parts with a high degree of precision and reduced scrap, or waste [9]. In addition, the utilization of a CAM process like AFP results in a digital twin, or stream of code that can be further analyzed for process optimization because the model generated in computer aided design (CAD) is verified in computer aided engineering (CAE) software. In addition, because the placement process is automated and controlled by the robot machine code, once the laminate and tooling have been designed in CAD and optimized with Finite Element Analysis (FEA) it can be downloaded to a CAM system like CGTech Vericut[®] software to validate the lay-up process for production. The use of laser heating is under development as a replacement for the traditional infrared heating source used in AFP of TS composites as industrial laser technology advances and is demonstrated to heat the material more rapidly and efficiently.

Laser-assisted AFP of CF reinforced thermoplastic slit-tape followed by a significantly faster laminate consolidation cycle in the autoclave is attractive from a production rate perspective [10]. To further reduce rate and the cost associated to operate and maintain the large, high-temperature autoclaves required to reach the T_M ($> 330^{\circ}\text{C}$) to fabricate PAEK thermoplastic parts, NASA and

Electroimpact, Inc.[®] (EI) have partnered to evaluate and develop the ICAT process to manufacture wing and fuselage skin for the next generation of commercial single-aisle aircraft.

1.2 Thermoplastic AFP Development Background

During the timeframe of 2004 to 2006, NASA partnered with Accudyne, Inc.[®] and the University of Delaware to develop the ICAT process under a NASA program to advance the technology of out-of-autoclave (OoA) aerospace composite structure fabrication [11,12,13]. Accudyne successfully delivered a gantry-style robotic automated tape placement (ATP) system capable of placing and consolidating flat quasi-isotropic thermoplastic matrix laminates [11]. The equipment utilized a hot gas torch (HGT) to heat the incoming tape and substrate ply above T_M and a heated, conformable area compactor to maintain the incoming tape and substrate above T_M long enough to establish intimate contact and polymer auto-hesion, or interdiffusion of polymer molecules across the interface between the plies. This configuration was found effective to supply enough heat energy to the CF/TP tape for auto-hesion and, in addition, a cooling area compactor was also needed to remove heat from the substrate and quench the material below T_M to prevent disbond of the interfaces after healing. While HGT is less efficient for heating the material than current industrial diode laser systems, it does have the advantage of heating the substrate layers above T_M several plies deep, and hence the need for the cooling compactor. ICAT trials with this equipment using Cytec[®] APC-2 (AS4/PEEK) 76-mm (3.0-in.) wide tape resulted in uni-directional laminates with short beam strength (SBS) and quasi-isotropic laminates with open hole compression (OHC) strengths as high as 80% of autoclave processed thermoplastic composites. The inability to reach equivalence with autoclave processed APC-2 laminates was attributed at the time to the quality of the supplied tape, which was intended for autoclave or vacuum-press fabrication [11]. According to reference [12], The high mechanical performance of laminates fabricated by Accudyne[®] and the University of Delaware may have been due to the use of multiple heated compaction steps by the ATP head after each ply was placed. The Accudyne[®] head successfully served as a test bed for ICAT process research and development, however its configuration was not deemed appropriate for high-rate production of complex curvature aircraft parts, such as wing and fuselage skin.

Since 2021, under the HiCAM project, NASA has partnered with EI to evaluate and develop the ICAT process using laser-assisted AFP equipment [13,14,15]. Recent advancements in industrial diode lasers have facilitated incorporation of laser heating as an alternative to the infrared heating systems commonly used to heat TS tape during the AFP of TS matrix composites. EI has developed a diode laser system powerful enough (≈ 400 Joule/sec.) to heat 2.54 cm wide courses of thermoplastic tape above the T_M at placement speeds in excess of 423 mm/sec (1000 in./minute). In contrast to the robotic gantry ATP system used by NASA and Accudyne[®] in previous ICAT studies, the EI thermoplastic AFP (TP-AFP) head is mounted on a six axis, or degree of freedom (6-DOF) Kuka Titan[®] robot, and the HGT is replaced with diode laser heating. The heated and cooling area compactors are replaced with a single room temperature conformable compaction roller made from flexible material capable of withstanding the high temperatures associated with ICAT. A series of ICAT processing characterization experiments were conducted [13, 14, 15] using the EI laser assisted TP-AFP head to determine the capability to place and heal the PAEK thermoplastic slit-tape materials, including Toray[®] T800/PEEK, Victrex[®] IM7/LM-PAEK, and Hexcel[®] IM7/PEKK. The short beam Strength (SBS) results of this effort are reported in [15] and

indicated that the ICAT fabricated panels did not achieve interlaminar strength comparable to the same materials fabricated in an autoclave.

The temperature profiles of the inter-ply region to be healed between the incoming tape and substrate ply was measured for each of these ICAT panels using a combination of forward looking infrared (FLIR) camera and thermocouples welded to the surface of the substrate ply [13,14]. The FLIR data measured the temperatures of both the incoming tape and the substrate tape surfaces just ahead of the compaction roller nip-point, where the two tapes come in contact as the compaction force is applied. The thermocouples measure the temperature of the inter-ply region and indicated that the processing times above the melt temperature of the polymer were less than a second as the two tapes were brought together under the compaction roller during the ICAT process.

NASA and EI completed ICAT processing experiments [13,14, 15] using PEEK, LM-PAEK and PEKK matrix CF reinforced tapes. SBS testing was conducted to determine the interlaminar strength of the ICAT 24-ply quasi-isotropic panels in comparison to panels fabricated in the autoclave. The highest SBS resulting from the ICAT PEEK panel was only 38% of the autoclave processed PEEK panel. This PEEK panel was fabricated using ICAT laser target temperature, $LT = 500^{\circ}\text{C}$, placement speed, $V = 100 \text{ mm/sec}$, and compaction load, $CL = 0.9 \text{ kN}$. The IM7/LM-PAEK panel was fabricated using a $LT = 475^{\circ}\text{C}$, $V = 400 \text{ mm/sec}$, and a $TT = 80^{\circ}\text{C}$. The average SBS of the LM-PAEK panel fabricated by ICAT was only 24% of the SBS of the LM-PAEK panel post-consolidated in the autoclave. The PEKK panels were fabricated using the same compaction load, a higher $LT = 525^{\circ}\text{C}$ and lower $V = 25 \text{ mm/sec}$ to increase the time the tape welding interface was above the PEKK $T_M = 332^{\circ}\text{C}$. The average SBS of the PEKK panels was only 16% of autoclave processed PEKK laminates. These results are contrary to the current understanding of auto-hesion and reptation theory [6]. A review of previous work in the literature on thermoplastic composite processing by Loos [19] and on the ICAT process by Agarwal [16], Pitchumani [18], and Gillespie [17,21] provide explanation for the poor mechanical performance resulting from the ICAT processing parameters used in the NASA test panels fabricated with EI. The low interlaminar strength of the PEKK panels is likely due to poor intimate contact between the tapes for this more viscous polymer using the 0.9 kN of compaction load and the short duration of the reptation time above T_M . Without sufficient intimate contact the thermoplastic molecules cannot inter-diffuse across the tape interfaces and auto-hesion is limited. Pitchumani and Ranganathan [20, 21] simplified a thermoplastic intimate contact mechanistic model developed by Dara and Loos [19]. The tape consolidation under the rollers is modeled as a squeeze flow continuum, in which the flow of the fiber/matrix is dependent on the process temperature, polymer viscosity, μ , and the tape fiber volume fraction. The degree of intimate contact, D_{IC} , at a given temperature T , compaction pressure, P , over the time integral that P is applied is then calculated using Equation 2:

$$D_{IC} = D_{IC0} \left[1 + C_1 \int_0^{t_P} \frac{P}{\mu_{mf}} dt \right]^{1/5} \quad (2)$$

Where, D_{IC0} is the initial degree of intimate contact and represents the area of contact between the two tapes just prior to compaction pressure application at the nip-point, at time $t_P = 0$. μ_{mf} is the viscosity of the fiber-resin mixture at the tape surface. μ_{mf} is calculated by multiplying the resin

viscosity, μ , by $1 / 1 - (\text{fiber volume fraction/packing factor})^{0.5}$. These relations are important to consider in understanding the poor SBS results NASA obtained from ICAT of the IM7/PEKK material. The PEKK material was processed at a slower speed and higher temperature than the T800/PEEK material to achieve longer time above the T_M , and greater auto-hesion, however the SBS results were only 18% of the autoclave processed PEKK laminate. Parallel plate rheology indicates that the PEKK polymer has a minimum melt-flow viscosity, $\mu = 850 \text{ Pa}\cdot\text{sec}$, at 370°C . In comparison, the PEEK polymer used in the Toray T800/PEEK tape has a measured minimum viscosity of $\mu = 205 \text{ Pa}\cdot\text{sec}$ at 390°C . According to Equation 2, a higher pressure is required to achieve the same D_{IC} in combination with additional time under the compaction roller to account for the higher viscosity of the PEKK polymer. The ICAT panel fabricated using PEEK achieved a higher degree of intimate contact above T_M using 0.9 kN of compaction force based on photo-microscopy of the panel, however the low interlaminar strength and the thermal history during ICAT indicate that the time above T_M was not sufficient to provide adequate molecular interdiffusion and auto-hesion according to the Gillespie non-isothermal welding model [17] and Agarwal's experimental work [16]. Agarwal verified Wool's isothermal welding model in Equation 1 with APC-2, reaching autoclave (hot-press) level interlaminar strength levels after only 7.0 seconds of isothermal welding time above the PEEK recrystallization temperature of 280°C [16]. In addition to isothermal welding experiments, Agarwal also conducted non-isothermal experimental analysis of thermoplastic tape interface welding during the laser assisted AFP process using a bench-top version of an AFP placement head to fabricate unidirectional SBS coupons using APC-2 tape. The resulting bond strength supports the predictive capabilities of the non-isothermal welding model developed by Bastien and Gillespie [18]. This welding model was based on Wool's polymer interdiffusion model, Equation 1, to predict the non-isothermal (transient) welding time of PEEK composite. The tube renewal time from reptation theory, τ_r , which, represents the amount of time required for complete welding at a temperature, T :

$$\tau_r(T) = \tau_r(T_{ref}) \exp \left[\frac{-E_a}{R} \left(\frac{1}{T} - \frac{1}{T_{ref}} \right) \right] \quad (3)$$

The activation energy E_a is calculated from an Arrhenius fit of experimental isothermal welding time versus temperature data and R is the universal gas constant. Using an $E_a = 57.3 \text{ kJ/mol}$ and $T_{ref} = 400^\circ\text{C}$, Agarwal calculated $\tau_r = 0.11 \text{ sec}$ for the PEEK polymer used in the APC-2 tape [16]. The Gillespie welding model [17, 18] is more appropriate to predicting the time required for auto-hesion during the transient thermal history of the ICAT process. Gillespie modified Equation 3, introducing a shift factor to obtain an equivalent degree of bonding achieved in the non-isothermal process [18]. The semi-empirical model in Equations 4 and 5 essentially map the non-isothermal process into a hypothetical isothermal process that would give an equivalent degree of bonding. Rewriting Equation 3 with τ_r expressed as an equivalent re-healing function based on an energy criterion:

$$\frac{G}{G_\infty} = \left(\frac{t_{eq}}{\tau_r(T_{ref})} \right)^{0.25} \quad (4)$$

Where, $\frac{G}{G_\infty}$ is the ratio of the energy release rate, G , at time t to the energy release rate of the fully healed PEEK polymer, G_∞ . The tube renewal time, τ_r , is calculated using Equation 2, and t_{eq}

represents the contact time necessary for an isothermal process at a reference temperature, T_{ref} , to obtain an equivalent degree of bonding as that achieved in the non-isothermal process.

$$t_{eq}^{0.25} = \sum_j \left[\left(\frac{t_j}{a(T_j)} \right)^{0.25} - \left(\frac{t_{j-1}}{a(T_{j-1})} \right)^{0.25} \right] \quad (5)$$

Where, a is the shift factor relating the non-isothermal model to the isothermal solution for τ_r . The shift factor is calculated from parameters found by fitting to the time at multiple temperatures from welding experiments [18]. The time interval, j , is summed from the temperature at the consolidation point to the crystallization temperature (280°C for PEEK). After calculating τ_r using Equation 2, the non-isothermal welding time, t_{eq} , to achieve different levels of strength can be calculated by solving Equation 3 and Equation 4, simultaneously. To validate Gillespie's thermoplastic welding model Agarwal utilized the bench-top laser-assisted AFP equipment to fabricate AS4/PEEK uni-directional test coupons by holding constant the speed and compaction pressure and varying the CO₂ laser power between 20 and 75 watts, resulting in maximum tape temperatures prior to compaction of 300°C to 475°C. The highest average SBS value of 49 MPa Agarwal reported was found using a speed of 15 mm/sec and laser power of 50 watts, which resulted in the incoming tape reaching a maximum temperature of approximately 475°C at the nip-point under a compaction pressure of 15.1 MPa. The Gillespie non-isothermal model and Agarwal's supporting experimental work with APC-2 PEEK tape predicts that the time required to achieve full auto-hesion for AS4/PEEK is 0.12 sec, which is only fractions of a second longer than the time above the T_M , that NASA and EI achieved during ICAT processing of PEKK [15]. The objective of the ICAT laser angle of incidence (AoI) study is to investigate the effects of varying the laser AoI on the time the tape interface to be welded is above T_M and thereby the in-situ strength development during the process. Based on thermal analysis [22] of the ICAT process, decreasing the laser AoI used on the EI head will increase the laser elliptical spot length, and accompanied by increased laser power, result in an increase in the time above T_M .

2. EXPERIMENTAL

The ICAT laser AoI study was conducted at EI using a six-axis Kuka Titan[®] robotic arm with an EI developed 6.35-mm (0.25-in.) tape, 8 lane (Q-8) placement head. The AFP head was configured to place 3.81-cm (1.5-in.) wide courses comprised of six 6.35-mm (0.25-in) wide carbon fiber reinforced thermoplastic slit-tapes onto a custom, 9.5-mm thick, aluminum tool. The flat tool was heated by a uniform hotplate supplied by Wencesco[®]. The EI VSS-HP laser heating system used in previous ICAT studies was mounted on the Q-8 head and configured to emit six 6.35-mm diameter circular spots (one for each tape), supplying up to 400 W per lane at a wavelength of 976 nm which could be controlled individually. At the normal AoI of 16° that the VSS-HP assembly is mounted on the head, the circular beam is incident on the substrate ply (tool surface) as an elliptical spot with a minor axis length of 6.35 mm and a major axis length of 11.5 mm. To increase the time that the tape interface to be welded is above the polymer T_M , the laser incident spot size was increased by decreasing the AoI on the substrate tape surface from the nominal 16° used in previous ICAT studies at EI to 14° and 12°. The most straightforward approach to changing the AoI of the EI VSS-HP laser assembly containing the sophisticated array of beam collimators and focusing mirrors was for EI to precision machine mounting brackets for the entire assembly. New mounting

brackets were machined to achieve the 14° and 12° AoI. These brackets also allowed fine-tuning of the angle within approximately $\pm 0.2^\circ$ to also affect the ratio of the spot length focused between the substrate tape on the tool and the incoming tape resting against the compaction roller as it travels toward the nip-point. The schematic shown in Figure 2 is the concept of the elliptical spot length change with varying AoI where the laser is incident at the start of the roller nip-point. The spot lengths associated with an AoI of 16° and 14° were calculated to be 11.5 mm and 14.1 mm, respectively as indicated in Figure 2 when 60% of the elliptical spot was focused on the substrate and 40% on the incoming tape, against the roller surface. The substrate length of the elliptical spot resulting from an AoI of 12° was calculated to be 21.0 mm. The decrease in AoI was limited to 12° because any further decrease would result in interference of the VSS-HP laser system assembly with the FLIR camera mounted to the AFP head directly behind the laser assembly, and for concerns of collision during AFP on contour parts.

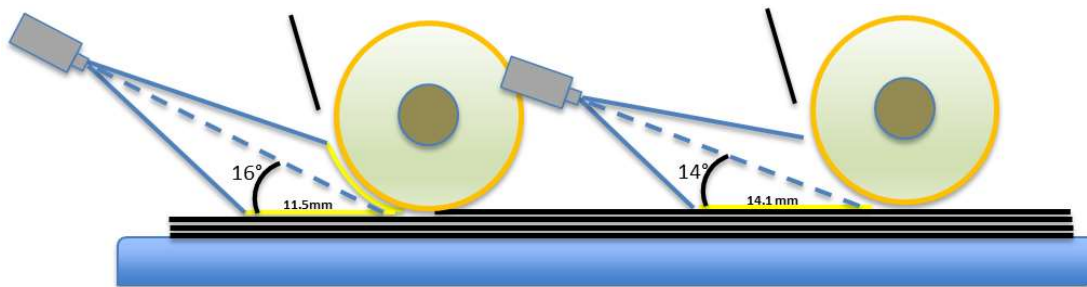


Figure 2. Schematic of ICAT laser angle of incidence .

Five, 50.8 cm \times 25.4 cm (20 in. \times 10 in.), composite panels with 24-ply, quasi-isotropic layups, [45/0/-45/90]_{3S}, were fabricated using Toray® T800/PEEK 6.35-mm (0.25-in.) wide slit-tape with the processing parameters shown in Table 1. In addition, a 24-ply quasi-isotropic panel, Panel #6, was fabricated using Victrex® IM7/LM-PAEK and Panel #7 of the study was fabricated using the LM-PAEK tape, but the lay-up was uni-directional [0]₂₄. Initially the plan was to fabricate all of the PEEK AoI panels using the same ICAT processing parameters of a target peak surface temperature (LT) of 525°C, a heated tool temperature (TT) of 180°C, placement speed (V) of 25 mm/sec, and with a compaction load (CL) of 1.5 kN (325 lbs.) and only vary the laser AoI used for each test panel. However, during placement of the first panel using an AoI of 16° and ratio of spot length between the incoming and substrate tape (I/S) of 60%/40%, respectively, the incoming tape stuck to the compaction roller wrapping around it instead of sticking to the substrate ply. This was the first instance of “roller-wrap” experienced during any of the ICAT trials conducted with EI and is assumed to occur because of the high LT and slow speed. This resulted in the incoming tape heating through the thickness so that the molten polymer stuck to the polyimide film coating on the high temperature conformable roller. The ICAT process was halted, and the LT was reduced to 500°C to place the panel using an AoI of 16° and the spot length ratio changed to I/S = 40/60 to reduce the time the incoming tape was exposed to laser heating. In addition to the parameters of LT and V causing the high temperature on the back-side of the incoming tape, the occurrence of roller-wrap also indicated that the previous assumption that heat was transferring to the relatively large mass of the roller from the relatively small mass of the tape were likely incorrect. The relationship of tape tension to the thermal contact between the incoming tape and the roller and the effect of this phenomenon on the thermal modelling are discussed further in [22].

As with previous ICAT studies conducted with EI, the laser power used for each panel was empirically determined in real-time using the FLIR image analysis software shown in Figure 3 at

each placement speed to produce the desired target surface temperature of the slit-tape. The data from the FLIR camera was also utilized during the ICAT process to measure the peak temperature reached. The rest of the thermal history, or temperature profile of the contacting tape interface, including under the compaction roller, was measured using a thermocouple welded to the top surface of the substrate tape at three different plies of the panel stack as shown in Figure 3-B. A thermocouple data acquisition (DAQ) system (NI[®] cDAQ-9174, CompactDAQ chassis equipped with a NI[®] 9212 8-Channel Module) capable of simultaneously measuring at 2,000 Hz, or samples per second per channel, was used to collect temperature measurements at the maximum sample rate during each 0° ply placement. The details of the temperature measurement procedure are explained in [13, 14].

Table 1. ICAT placement parameters and target AoI conditions.

Slit-tape Material	Panel #	Targeted AoI (degrees)	LT (°C)	V (mm/sec)	TT (°C)	CL (kN)	Targeted Spot Length Ratio of Incoming to Substrate Tape
PEEK	1	16	500	25	180	1.5	40/60
	2	14	500	25	180	1.5	50/50
	3	14	525	25	180	1.5	40/60
	4	12	525	25	180	1.5	50/50
	5	12	525	25	180	1.5	40/60
LM-PAEK	6	12	450	80	180	1.5	40/60
	7	12	450	80	180	1.5	40/60

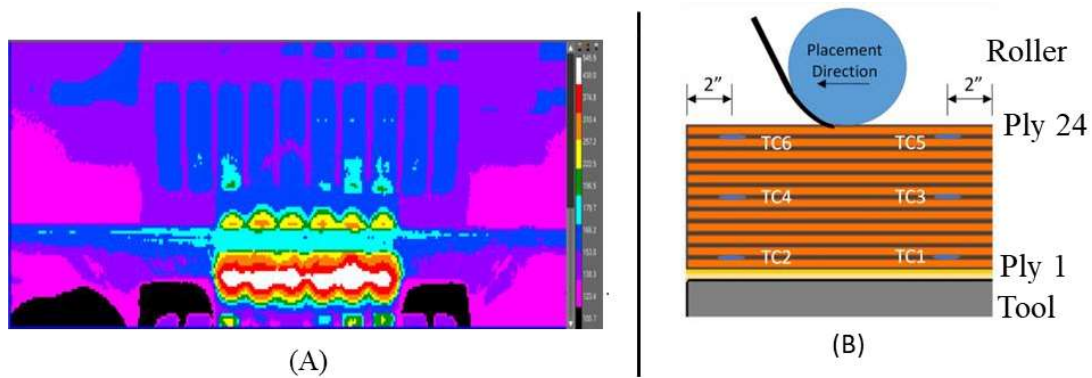


Figure 3. ICAT temperature profile measurements using (A) FLIR camera imaging (AoI Panel #5 placement shown) and (B) thermocouples placed at various locations of each panel ply-stack.

The laser AoI and the ratio of the elliptical spot length focused on the incoming and substrate tape just ahead of the roller nip-point were measured using Edmunds Optics Zap-It[®] laser alignment burn paper. To ensure that the VSS-HP system mounting brackets were providing the target AoIs of 16°, 14°, and 12°, the laser target paper was affixed to a 90° (relative the tool plate) bracket and

the lasers were energized for approximately 0.03 sec. The robot was then moved horizontally 70 mm away from the target and the laser energized again. The vertical distance between the spots on the burn paper (as measured by calipers) and the horizontal distance the robot was moved (70 mm) was used to calculate the angle of incidence [$\theta = \text{atan}(\Delta y / \Delta x) = \text{atan}(\Delta y / 70 \text{ mm})$]. The ratio of the elliptical spot focused only on the substrate versus the incoming tape was also measured using the laser alignment paper. In this case, the paper was adhered to the flat tool and the roller was left in place with the surface shielded so that when the laser was energized it left burn marks only corresponding to the laser spot on the substrate (tool). The roller was then removed and the full projection of the lasers onto the tool plate was also measured using the alignment paper. After the AoI study was completed at EI, the laser target papers were labelled and returned to NASA, where they were scanned, and measured using digital image analysis software. The digital images of the laser alignment paper with the elliptical burn marks when the AoI = 12° for the six spots incident on the substrate (A) and the portion of the elliptical burn marks when the AoI is 12° and 60% of the spot length is incident on the substrate (B) are shown in Figure 4.

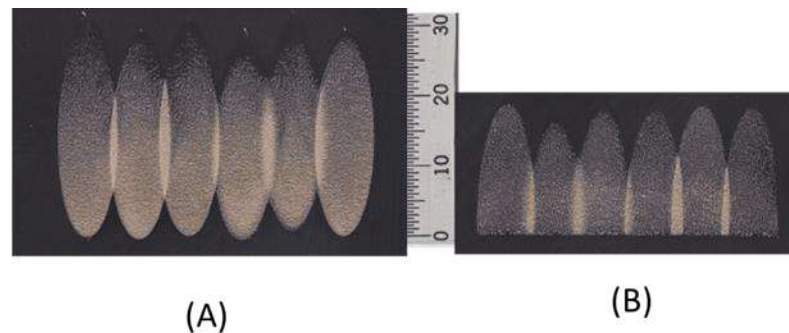


Figure 4. Images of laser alignment paper burn marks next to a mm scale for (A) six lasers incident on the flat tool with roller removed and (B) six laser spots incident on the substrate only.

After ICAT of the seven AoI panels at EI, each of the 51 cm × 25 cm (20 in. × 10 in.) quasi-isotropic test panels were shipped to NASA for further processing and evaluation. At NASA, each panel was machined into three 10 cm × 25 cm (4 in. × 10 in.) sections and returned to the NASA advanced composites processing lab for post-consolidation and NDE. One of the sections from each of the seven AoI panels was labelled “ICAT-Only” and received no further post-ICAT consolidation step. One of the sections was post-consolidated in the autoclave using the material supplier recommended cycle for PEEK of 390°C hold for 30 minutes under 690 kPa gauge pressure (100 psig) and full vacuum. The third section from each of the AoI panels was post-consolidated using a vacuum bag only (VBO) process. For the five PEEK AoI panels, the VBO cycle included a 390°C hold for 30 minutes under full vacuum. The two LM-PAEK AoI panels were post processed in the autoclave (“ICAT + autoclave”) and VBO (“ICAT + VBO”) using a different temperature cycle, including a 60 min hold at 360°C under 690 kPa gauge pressure (100 psig) in the autoclave and full vacuum in the VBO process. The material supplier claims that the LM-PAEK polymer composite material can be consolidated at temperatures as low as 360°C, and therefore these two panels were consolidated at this lower hold temperature to determine the validity of that claim. The goal is to be able to reach autoclave equivalent mechanical performance

using either ICAT-only or by VBO post-lay-up consolidation at the lowest processing temperature and least amount of hold-time. After each panel section had been post-consolidated, the three sections underwent NDE by ultrasonic testing (UT), prior to machining by wet-saw (grinder) for SBS coupon prep according to ASTM D2344. Approximately sixteen 2.54 cm × 0.635 cm (1 in. × 0.25 in.) SBS coupons were cut from each of the three panel sections. According to the ASTM standard the length and, especially, the width of the coupon is dictated by the thickness of the panel section. In all cases the autoclave post-processed panel sections were slightly thinner by approximately 0.0051 mm (0.002 in.) than the ICAT-only and VBO post-consolidated sections. One of the SBS coupons from each panel section was polished and photo-micrographed to determine consolidation quality while the rest of the coupons were tested in SBS to determine the processing effects on the interlaminar strength (ILS) of the laminate.

3. RESULTS AND DISCUSSION

The measurement of the laser elliptical spot size resulting from the different AoI utilized during the ICAT study was conducted at NASA using digital analysis software. Images of the burn marks for the six elliptical spots from AoI of 12° are shown in Figure 4. The average values measured in the image analysis of the entire laser elliptical spot length as well as the portion of that spot length which was only incident on the substrate are listed in Table 2. Based on the values of lengths measured, the actual AoI and the ratio of the laser spot length (Spot Ratio) focused on the incoming tape vs. substrate tape was calculated and is also indicated in Table 2.

Table 2. Measured laser elliptical spot sizes and corresponding calculated AoI and spot ratio.

Slit-tape Material	Panel #	AoI (degrees)	Spot Ratio Incoming/Substrate	Laser Spot Length (mm)	Substrate Only Spot Length (mm)
PEEK	1	16 ± 0.3	40/60	26.6 ± 0.8	15.9 ± 0.4
	2	14 ± 0.3	53/47	30.6 ± 1.0	14.3 ± 0.6
	3	14 ± 0.3	40/60	35.0 ± 1.0	18.0 ± 0.7
	4	12 ± 0.3	54/45	33.7 ± 1.3	16.0 ± 0.9
	5	12 ± 0.3	37/63	33.7 ± 1.3	21.3 ± 0.6
LM-PAEK	6	12 ± 0.3	37/64	33.7 ± 1.3	21.3 ± 0.6
	7	12 ± 0.3	37/65	33.7 ± 1.3	21.3 ± 0.6

The average measured laser spot lengths in Table 2 correspond well with the intended, or planned, target values for AoI listed in Table 1. The spot ratios (SR) calculated from the substrate-only spot lengths indicate two distinct treatments of I/S ratio of laser heating energy focused on the incoming tape / substrate tape prior to these two tapes contacting and forming the welding interface under the compaction roller (approximately 50/50 and 40/60). For example, of a 40/60 I/S ratio, if the total projection of the laser is 30.0 mm, then the spot length on only the substrate would be 18.0 mm.

The temperature profiles, or thermal history, of the PEEK tape surfaces during the ICAT process are displayed in the plots in Figures 5. The experimental data for thermocouple #3 (TC3) in all

cases and the temperature profile predicted by the NASA developed one dimensional (1-D) closed-form thermal model [22] for comparison are shown in Figure 5. The model predictions were utilized to plan the study. Both the predicted thermal response as well as the empirical data indicate the small increase in time above T_M (weld-time) as the AoI decreases from 16° to 14° and 12° and the laser spot size increases. The experimental data appears to indicate that the 14° and 12° AoI treatments result in similar weld time, however Panel #2 with an AoI of 14° and an I/S of 53/47 was placed using a LT of 500°C , while Panel #4 with AoI of 12° and I/S of 54/45 was placed using an LT of 525°C , hence somewhat confounding the experimental data. This difference in the peak temperature is captured in the curve.

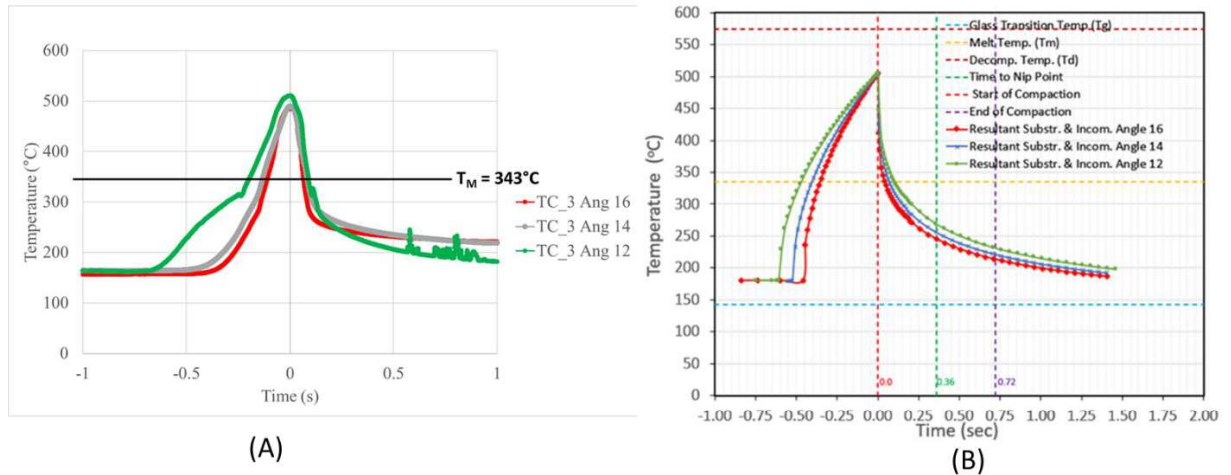


Figure 5. Temperature profile of each AoI with an I/S of 50/50 for the PEEK panels (A) measured and (B) 1-D model predictions for the same conditions.

The measured temperature profiles from the FLIR camera and the four thermocouples located in the substrate ply stack (away from the heated tool) for each of the six quasi-isotropic panels were analyzed and the average weld-time was calculated according to the time above the T_M of 343°C and T_M of 305°C for PEEK and LM-PAEK, respectively. The chart in Figure 6 shows the expected trend of increasing weld-time with increasing laser spot size. As expected, the longest weld-time was achieved for Panel #4 using an AoI of 12° and the ratio of the spot length (I/S) of 54/45. Again, this panel was placed using a LT of 525°C in contrast to Panel #1 and #2 which were placed using an ST of 500°C to prevent roller-wrap. The relatively lower average weld-time of the LM-PAEK panel is due to the higher V of 80mm/sec, and the lower LT of 450°C corresponding to the lower T_M for this material. The purpose of Panel #6 was to demonstrate that an ICAT process using more optimum AoI, and higher placement rates could achieve autoclave level interlaminar strength and meet placement rate objectives. After the ICAT panels were fabricated at EI, they were machined into three sections. Two of these panel sections were post-processed in either an autoclave or in an oven by the VBO process. The three panel sections then underwent non-destructive inspection (NDI) by an ultrasonic technique (C-scan). The results of the C-scan of each AoI panel are shown in Figure 7. The C-scan image contains all three panel sections, including the autoclave post-processed section on the top, “ICAT-Only” in the center and the VBO section on the bottom, as labelled. The NDI indicates that all three of the “ICAT-Only” panel sections have elevated porosity in comparison to the autoclave and VBO-post-processed panel sections. However, the highest

signal loss occurred in C-scan of Panel #4 which was ICAT processed with the longest weld-time. A poor C-scan result is typically an indication of poor intimate contact between plies. The best “ICAT-Only” result in C-scan for all six of the panels was the LM-PAEK Panel #6 with an AoI of 12°, which had low signal loss, comparable to the autoclave consolidated panel sections. In contrast to the NDI results, the photo-microscopy of all the panel sections indicate that intimate contact was established, at least in the region from which photo-microscopy specimens were obtained (in the middle of each panel section).

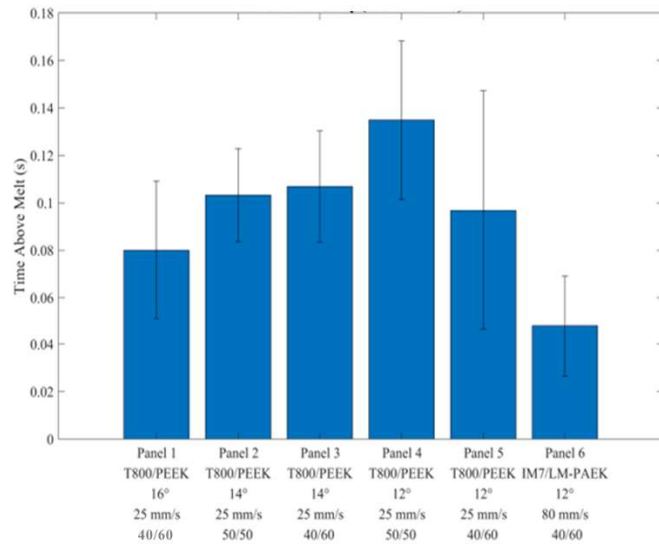


Figure 6. Average weld-time (time above T_M) for the five PEEK and one LM-PAEK AoI panels.

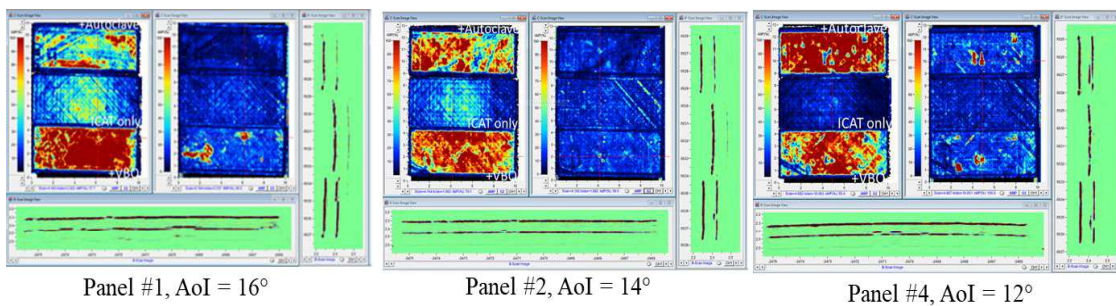


Figure 7. Result of NDI (C-scan) of PEEK ICAT Panels Fabricated Using the Nominal Spot Ratio, I/S = 50/50 and AoIs of 16°, 14°, and 12°.

Photo-micrographs of all of the AoI panel sections were taken at 200X magnification after machining and polishing one of the SBS coupons from the center of each panel section. All of the images indicated less than 2% by volume porosity. The “ICAT-only” panel sections did show some porosity in both the inter-ply and intra-ply regions. Figure 8 is the photo-microscopy for Panel #4, shown for comparison to the C-scan image in Figure 7, which indicated high void content. The image in Figure 8 is representative of all of the panel sections inspected by microscopy. The “ICAT-Only” section in Figure 8 does not indicate a level of inter-ply porosity that would explain the poor C-scan results shown for this same panel in Figure 7. The most likely

reason is that the photo-microscopy was not taken in sections where higher void content is indicated by the ultrasonic inspection. In addition, none of the panel sections scanned by UT were entirely flat. Even with these techniques, the degree of auto-hesion, or in-situ strength development achieved between plies in a thermoplastic composite, must be determined by mechanical testing of the composite laminate especially during process development.

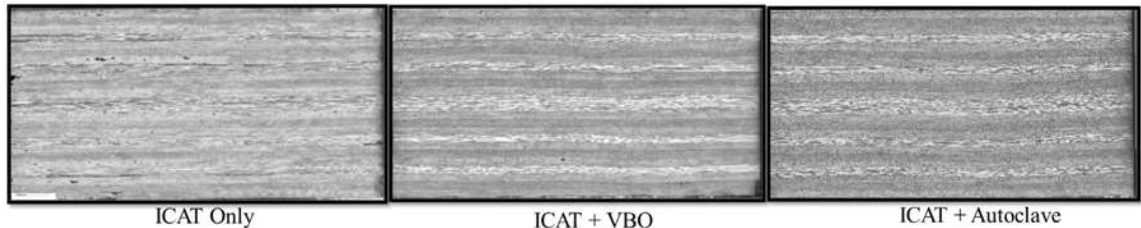


Figure 8. Photo-micrographs of PEEK Panel #4 (AoI = 12°) at 200X magnification.

The results of SBS testing of all the AoI panels fabricated by ICAT as well as the post-processed panel sections are shown in Figure 9. Each normalized average SBS strength value reported is based on an average of five coupon valid ILS failures according to ASTM D2344. All values have been normalized as a percentage of the average SBS of the autoclave processed T800-PEEK Panel #1. Most of the SBS coupons from the autoclave post-processed panels regardless of ICAT process parameters or tape material failed with an average SBS which was statistically equivalent, or within the standard deviation.

Both the “ICAT-Only” and the “ICAT + Autoclave” coupons from the LM-PAEK uni-directional [0]₂₄ Panel #7 failed with significantly higher average SBS strength than the quasi-isotropic PEEK Panels #1-#5 and the LM-PAEK Panel #6 fabricated using the same ICAT process parameters. Panel #7 was fabricated and tested due to concern over the SBS results in the literature by other groups currently developing the ICAT process for the PAEK polymers. In most cases, these groups report achieving “ICAT-Only” over 50% interlaminar strength of autoclave, or press, fabricated laminate because they are testing uni-directional laminates. The carbon fiber reinforcement in uni-directional thermoplastic laminates tend to nest under compaction load, resulting in less well-defined interlaminar zones between plies. This nesting phenomenon, evident in photo-microscopy, results in higher SBS values and confounds the effects of processing. The ASTM for SBS certainly allows for testing of uni-directional laminates, however the results for Panel #7 certainly confirms the concern that the results reported by other groups may be misleading. Aircraft parts, especially primary structure are fabricated using quasi-isotropic laminates, not uni-directional laminates.

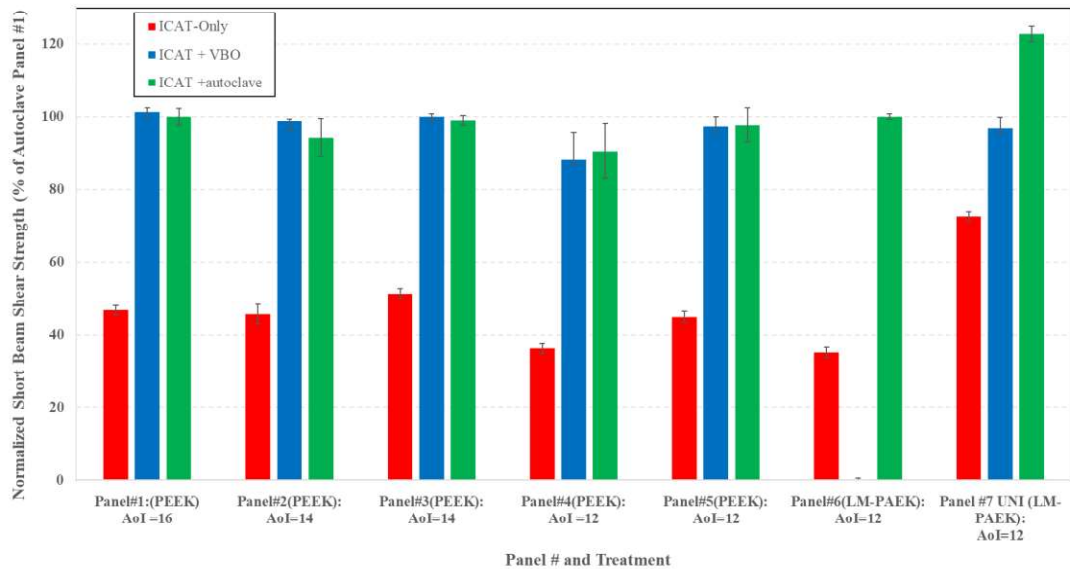


Figure 9. SBS strength of AoI Panels #1-#7, normalized as a percent of the autoclave post-processed Panel #1.

The comparison between the average weld-times reported in Figure 6 with the results of the SBS testing in Figure 9 does not clearly match with the current understanding of reptation theory and the relationship between auto-hesion and weld-time. All of the PEEK ICAT panels tested in the AoI study exceed the results from the previous ICAT study with the T800/PEEK slit-tape where the average SBS strength was only 38% of the autoclave post-processed panel. ICAT Panel #3 fabricated using an AoI of 14°, has a higher SBS than Panel #1 using an AoI of 16°, which agrees with the expected trend, since the average weld time for Panel #3 was 0.02 sec longer than Panel #1. However, based on this trend, Panel #4 which was processed with the longest measured average weld-time should have exhibited the highest interlaminar strength. Instead, Panel #4 had a lower SBS strength than Panels #1, #2, and #3. Further, the C-scan results for Panels #1 and #2 were comparable, while the NDI of Panel #4 indicated elevated porosity. The most likely cause of this unexpected result is that the ICAT processing temperature of 525°C used for Panel #4 is resulting in degradation of the PEEK polymer on the tape surface. The temperature used to process this panel is well below the reported 2% mass-loss decomposition temperature of 575°C reported for PEEK [12,16]. The literature is unclear on the effects of extremely short dwell times (0.01 sec) at the elevated temperature of 525°C reached during the highly transient heating and cooling of the tape surfaces during laser-assisted AFP (Figure 5), however it is certainly possible that scission of the PEEK molecule is occurring. If the polymer is degrading, or breaking into shorter molecular chains, its ability to inter-diffuse across the inter-ply boundary will be limited. Chain scission would not explain poor intimate contact that the NDE results seem to indicate. The effects of varying the ratio of the laser spot length between the incoming tape and the substrate tape was not as clear as originally expected. These results are likely confounded by the decision to reduce both the LT from 525°C to 500°C and the I/S ratios of Panels #3 and #5 from the intended I/S of 60/40 to an I/S of 40/60. This was deemed necessary to prevent the roller-wrap issue from reoccurring after the incident with Panel #1. The roller-wrap that did occur provided a key learning about the degree of thermal contact between the incoming tape and the compaction roller, just ahead of the

nip-point and during the laser heating of the incoming tape. The low tensile force applied to the incoming tape (typically, ≤ 40 N) is not high enough to establish good thermal contact, in contrast to the compaction force under the roller (around 1.5 kN). Therefore, the heat transfer from the incoming tape into the large thermal mass of the roller is limited and, contrary to the original assumption, the incoming tape can reach the process target temperature with a smaller spot length. This is supported by the higher SBS result for Panel #3 (I/S ratio of 40/60) in comparison to Panel #2 (I/S ratio of 50/50). The same trend was observed for the AoI of 12° for Panel #5 in comparison to Panel #4. In addition to seeking to improve the strength developed in-situ during the ICAT process, the AoI study results were intended to add to the current understanding of the weld-time required to reach full auto-hesion during the process. Figure 10 is a plot of the Gillespie semi-empirical welding model (Equations 4 and 5) developed for non-isothermal processes like ICAT. The curve was generated based on data collected by Agarwal [16]. The strength results from the ICAT AoI panels are also plotted as individual points (squares) for comparison of the current results to the model. The weld-times and associated SBS strength ratios calculated for the NASA ICAT of T800/ PEEK quasi-isotropic differ from the model in magnitude and the NASA AoI data does not fit a trend like Agarwal's data collected using the bench-top laser-assisted AFP equipment to fabricate and test uni-directional SBS coupons. The advantage of testing uni-directional SBS coupons in comparison to quasi-isotropic coupons has already been addressed. Another likely reason for the poor fit to the Gillespie thermoplastic laminate welding model [18] may also be due to the high compaction pressure (15.2 MPa) used in the Agarwal ICAT process versus the approximate 9 MPa used in the ICAT process of the NASA panels. The compaction pressure would not directly affect the calculation of the equivalent time, t_{eq} , plotted in Gillespie's model curve, however it would affect the degree of intimate contact calculated using the Loss model [19]. The degree of intimate contact and the auto-hesion time predicted by Gillespie's model are coupled, because auto-hesion cannot proceed without good intimate contact between the surfaces to be welded. In addition, and of less importance, is that the activation energy, E_a , of the APC-2 material used in Agarwal's coupons has been calculated to be 57.3 kJ/mol, whereas the activation energy of the Toray PEEK polymer has not been characterized and is likely different.

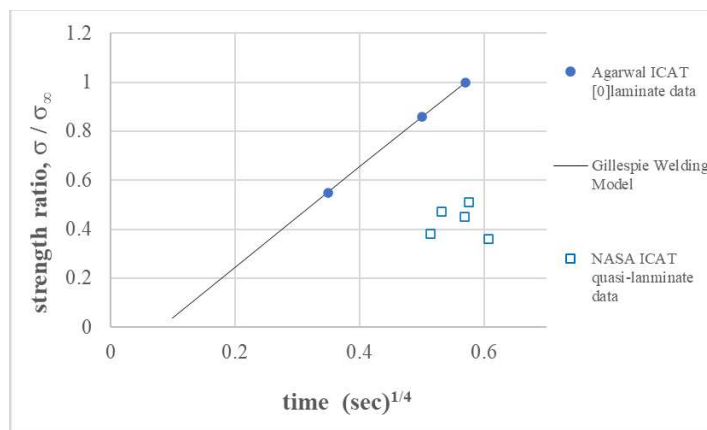


Figure 10. Comparison of NASA T800/PEEK ICAT-AoI quasi-isotropic SBS strength data (blue squares) to the Gillespie Welding Model and APC-2 unidirectional strength data from Agarwal [16].

4. CONCLUSIONS

The AoI study was intended to investigate the effects of reducing the AoI from 16° to 14° and 12° on the time above the polymer T_M during the ICAT process and to understand the effect of focusing more of the laser energy on the incoming tape and less on the substrate tape. The results indicate that increasing the laser spot length by decreasing the AoI did increase the time the interface to be welded was above the polymer T_M . However, the trend expected based on polymer reptation theory was not strongly supported by the results of the SBS testing. The strength did increase when the AoI was reduced from 16° to 14°, but the same trend was not observed for the Panel #4 with an AoI = 12° that was above the PEEK T_M for the longest average time. A straightforward explanation for this is confounded by the fact that a higher laser target temperature of 525°C was used in the ICAT process for Panel #4 and #5 than was used for Panel #1 and #2. The higher temperature increased the weld-time, but it may have also initiated degradation of the PEEK polymer. Plotting the resulting AoI study strength vs. weld-time and comparing it with a semi-empirical thermoplastic welding model indicates the resulting values are comparable in magnitude but the strength versus weld-time data from the AoI study do not match the predicted trend for other PEEK composites fabricated by other institutions. Current models for consolidation of thermoplastic composites are based on intimate contact between plies and molecular interdiffusion. Intimate contact is a function of surface roughness and is achieved through resin flow, while molecular interdiffusion produces molecular entanglements across the bonding interface and is responsible for most of the interfacial strength. More work is recommended, especially the characterization of the degree of decomposition for PAEK polymers subjected to highly transient heating and cooling regimes. The AoI study demonstrated that the incoming tape can be heated using smaller laser spot lengths (i.e., less laser energy) because the thermal contact between the incoming tape and the compaction roller is not high enough to facilitate a high heat flux value (i.e., heat transfer into roller is slower than originally assumed). Lastly, the SBS results for the unidirectional LM-PAEK (Panel #7) outperformed all other panels fabricated by ICAT, not because of the processing parameters or the AoI, but because SBS testing of unidirectional thermoplastic composites results in higher strength due to fiber-nesting that cannot occur in quasi-isotropic thermoplastic composites. The ICAT laser angle of incidence study resulted in several key, albeit minor, learnings about the process. It is the opinion of the authors that thermoplastic composites and the ICAT process are the future of aerospace structure fabrication for the advantages discussed but especially because the process enables fabrication of large light-weight structure out of the autoclave, which will enable future aircraft design and manufacture beyond the current tube with wings paradigm. Blended wing body, large space launch, interplanetary craft, and especially in-space or at destination (e.g., moon or Mars) composites fabrication would benefit from further development of the ICAT process. Therefore, it is recommended that the decomposition initiation temperature of the PAEK polymer under transient heating be definitively characterized. With that information a more robust study of the welding time required to fully heal the PAEK interface should be conducted. With those critical parameters established, the thermoplastic AFP equipment can be designed to facilitate the optimization of the ICAT process.

5. REFERENCES

1. Lian, E, Lovingfoss, R., and V. Tanoto; "Qualification Material Property Data Report of Medium Toughness PAEK thermoplastics Toray (Formerly TenCate) Cetex TC1225 (LM PAEK) T700GC 12K T1E Unidirectional Tape, 145 gsm 34% RC," NCAMP Test Report Number: CAM-RP-2019-036 Rev A; 2021
2. O'Brien, T.K., and R.H. Martin; "Round-Robin Testing for Mode I Interlaminar Toughness of Composite Materials," *Journal of Composites Technology & Research*, Vol. **15**, No. 4, 1993, pp. 269-281. DOI: 10.1520/CTR10379J
3. Corveleyn, S., Lachaud, F., Berthet., F., and C. Rossignol; "Long-term creep behavior of a short carbon fiber-reinforced PEEK at high temperature: Experimental and modeling approach," *Journal of Composite Structure*, Vol. **290**, 15 June 2022, doi.org/10.1016/j.compstruct.2022.115485
4. Rubin, A.M., Fox, J.R., and R.D. Wilkerson; "Continuous Molding of Thermoplastic Laminates," U.S.Patent Application Publication# 20110206906A1, The Boeing Company, 2011.
5. Dara, P.H. and A.C. Loos; "Thermoplastic Matrix Composite Processing Model," Graduate Dissertation, Virginia Polytechnic Institute, CCMS-85-10, 1985.
6. P.C. deGennes; "Reptation of a Polymer Chain in the Presence of Fixed Obstacles," *Journal of Chemical Physics*, VOL:55, No.572 (1971); DOI: 10.1063/1.1675789
7. Wool, R. P. and O'Conner, K. M., "A Theory of Crack Healing in Polymers," *Journal of Applied Physics*. 52(10), p.5953-5963, 1981
8. Wool, R. P. and O'Conner, K. M., "Time Dependence of Crack Healing," *Journal of Polymer Science. Polymer Letters Edition*. Vol **20**, p.7-16,1982.
9. Donough, M.J., Shafaq, St.John, N.A., Phillip, A.W., and B.G. Prusty; "Process modelling of In-situ Consolidated Thermoplastic Composite by Automated Fibre Placement – A review,"- *Journal of Composites: Part A*, Vol163,(2022),DOI: doi.org/10.1016/j.compositesa.2022.107179.
10. Heil, Joseph P.; Wadsworth, Mark A.; Dando, Kerrick R.; Jones, Ron E.; Tymes, Matt; Slater, Sam J.; Bahr, Rodney E.; Bearden, Bryan T.; "Thermoplastic Composite Rate Enhanced Stiffened Skin: A Case Study," *SAMPE Journal*, Vol. 59,p.9, (2023), DOI: 10.33599/SJ.v59no6.01.
11. Lamontia, M. A., Gruber, M. B., Waibel, B. J., Cope, R. D., and A. B. Hulcher, "Conformable Compaction System used in Automated Fiber Placement of Large Composite Aerospace Structures," *Proceedings of the 23rd SAMPE EUROPE Conference*, (2002); DOI: 20030065867.
12. Tierney, J., and J. W. Gillespie, Jr; "Modeling of In Situ Strength Development for the Thermoplastic Composite Tow Placement Process," *Journal of Composite Materials*, Vol 40, No. 16, (2006); DOI:10.1177/0021998306060162.
13. Grimsley, B.W., Cano, R.J., Hudson, T.B., Palmieri, F.P, Wohl, C.J., Ledesma, R.I., Sreekantamurthy, T., Stelter, C.J., Assadi, M.D., Jordan, R.F., Rower, J.H., Edahl, R.A., Shiflett, J.C., Connell, J.W., and Brian J. Jensen; "In-Situ Consolidation Automated Fiber Placement of Thermoplastic Composites for High-Rate Aircraft Manufacturing," *SAMPE Conference*, May 2022. ISBN: 978-193455141-7.
14. Hudson, T. B., C. T. Dolph, G. M. Grose, R. J. Cano, R. F. Jordan, C. J. Wohl, R. I. Ledesma and B. W. Grimsley, "Thermal Response of Thermoplastic Composite Tape During In-situ Consolidation Automated Fiber Placement Using a Laser Heat Source," in *SAMPE 2023*, 2023. doi:10.33599/nasampe/s.23.0101.
15. Cano, R.J., Grimsley, B.W., Hudson, T.B., Shiflett, J.C., Wohl, C.J., Ledesma, R.I., Sreekantamurthy, T., Stelter, C.J., Kang, J.H., Nancarrow, J.P., Jordan, R.F., and J.H. Rower; "Composites from In-situ Consolidation Automated Fiber Placement of Thermoplastis for High-rate Aircraft Manufacturing," *SAMPE Conference*, May 2024 (in-press).
16. Agarwal, V.; "The Role of Molecular Mobility in the Consolidation and Bonding of Thermoplastic Composite Materials," Doctoral Dissertation, The University of Delaware; (1991).
17. Agarwal, V., S. I. Guqeri, R. L. McCullough and J. M. Schultz; "Thermal Characterization of Laser-Assisted Consolidation Process," *Journal of Thermoplastic Composite Materials*, Vol 5, No. 2:pp115-135, (1992). DOI:10.1177/089270579200500203
18. Bastien, L.J., and J.W. Gillespie; "A Non-Isothermal Healing Model for Strength and Toughness of Fusion Bonded Joints of Amorphous Thermoplastics," *Polymer Engineering and Science*, , Vol. **31**, No. 24; pp.1720-1730.(1991); DOI: 10.1002/pen.760312406
19. Dara, P.H. and A.C.Loos; "Thermoplastic Matrix Composite Processing Model," Virginia Polytechnic Institute, CCMS-85-10. (1985)

20. Yang, F. and R. Pitchumani; “Nonisothermal Healing and Interlaminar Bond Strength Evolution During Thermoplastic Matrix Composites Processing,” *Journal of Polymer Composites*, Vol. **24**, No. 2; pp: 263–278; (2003); DOI:10.1177/0021998306060162
21. Pitchumani, R., Don, R.C., Gillespie, Jr., J.W. and S. Ranganathan; “Analysis of On-Line Consolidation during the Thermoplastic Tow-placement Process,” Book Chapter In: Alam, M.K. and Pitchumani, R. (eds), Heat and Mass Transfer in Composites Processing, ASME Press. (1994).
22. Stelter, C.J., Sreekantamurphy, T., Hudson, T.B., and B.W. Grimsley; “Thermal Modelling of the In-situ Consolidation of Automated Fiber Placement of Themoplastic Composites,” SAMPE Conference, May 2024 (in-press).